

Crustal Compensation during Mountain-building

Shijie Zhong¹ and Maria T. Zuber

Department of Earth, Atmospheric and Planetary Sciences, Massachusetts Institute of Technology, Cambridge

Abstract. Airy isostasy has been observed in many active orogenic regions including Himalayas/Tibetan plateau and Tian Shan. To better understand the temporal evolution of mountain building, we investigate how topography at the surface and crust-mantle boundary (*i.e.*, Moho) that evolves in response to crustal shortening depends on mechanical properties of continental lithosphere. Our dynamic models reveal that if the effective viscosity of continental lithosphere is less than 100 times of the viscosity of the underlying mantle, orogenic belts and their corresponding roots at Moho can grow simultaneously with the Airy isostasy being approximately maintained. This result is consistent with the relatively small viscosity inferred for continental lithosphere of actively deforming central Asia regions including Tibetan plateau.

1. Introduction

Distinct topographic features on continents including orogenic belts are dominated by variations in crustal thickness through isostatic compensation. The original models of Airy and Pratt isostasy were based on the Archimedean principle and imply a static balance of pressure in crustal columns, with the balance in the Airy mechanism occurring by crustal thickness changes while that in the Pratt case is accomplished by lateral density variations. Gravity, topography, and seismic observations indicate that regions of active orogeny including the Himalayas/Tibetan plateau and Tian Shan are approximately isostatically compensated [Jin et al., 1996; Burov et al., 1990] while many tectonically stable and old orogenic belts including the southern Appalachians [McNutt, 1980] and Caledonia [Kusznir and Matthews, 1988] show significant isostatic gravity anomalies. Deviations from local isostasy for inactive orogenic belts can be attributed to the combined effects of dynamic compensation processes immediately following orogeny that lead to non-isostatic states [Zhong, 1997] and subsequently increased lithospheric strength which is capable of supporting deviatoric stresses indefinitely on a regional scale [Daly, 1940].

The purpose of this paper is to examine the relationship between crustal compensation and mechanical structure of continental lithosphere during the mountain-building. The common paradigm for mountain-building is crustal shortening [Dewey et al., 1973; Molnar and Tapponnier, 1975; England and McKenzie, 1982], although detachment of lithospheric roots due to convective erosion may play a role in certain stages of the process [Fleitout and Froidevaux, 1982; Houseman et al., 1981]. Geological observations and geodetic measurements of crustal deformation have confirmed the

essential role of crustal shortening or convergence in building the Himalayas/Tibetan plateau [e.g., England and Molnar, 1997] and Tian Shan [Abdrakhmatov et al., 1996]. In comparison to the deformation of oceanic lithosphere, deformation of the crust is distributed broadly in these orogenic belts and the velocity of crustal convergence appears continuous [England and Molnar, 1997], though there are regional concentrations of deformation associated with pre-existing lithospheric heterogeneity and loci of complex plate forces. England and Molnar [1997] have demonstrated that the measured strain field of crustal deformation in central Asia can be related to gravitational potential energy (*i.e.*, crustal density structure) via the Stokes' equation and that the average viscosity for continental lithosphere in central Asia is around 10^{22} Pa.s. In this paper, we explore simple dynamic models to understand the crustal compensation processes in continental lithosphere that undergoes uniform crustal shortening and their relationship to mantle and continental lithosphere viscosity structure

Physical Models

Our analysis represents the further development of a previous crustal compensation formalism [Zhong, 1997]. The model contains two assumptions. First, the crust and mantle have a layered and linear viscoelastic rheology and are incompressible. Second, amplitudes of topography at surface and Moho are significantly smaller than the most significant wavelengths of topography. With these two assumptions, the conservation equations of mass and momentum can be solved analytically to predict the time evolution of surface and Moho topography in response to crustal shortening. Conservation equations of mass and momentum are

$$\nabla \cdot \vec{u} = 0, \quad (1)$$

$$\nabla \cdot \hat{\sigma} - \rho g \vec{e}_z = 0, \quad (2)$$

where ρ , g , and $\hat{\sigma}$ are the density, the acceleration of gravity, and the stress tensor, respectively, $\vec{u} = (u_x, u_z)$ is the flow velocity, and \vec{e}_z is upward-directed unit vector. Contributions from internal density interfaces and time dependence via a Maxwell rheology enter the analysis through the density and stress tensors:

$$\rho = \rho_i + \delta\rho, \quad (3)$$

$$\hat{\sigma} + \frac{\eta}{\mu} \frac{d\hat{\sigma}}{dt} = -p\hat{I} + \eta\nabla\vec{u}, \quad (4)$$

where ρ_i is the average density for the i^{th} layer, $\delta\rho$ is the density anomaly, t is the time, μ is the shear modulus, η is the dynamic viscosity, p is the pressure, and \hat{I} is the identity matrix. Interface topography can be directly related vertical velocity on each boundary by using kinematic conditions. After eliminating the hydrostatic pressure in the stress tensor in (2), the system of equations is solved by using a Laplace transform technique [Zhong, 1997].

¹Now at Department of Physics, University of Colorado, Boulder, Colorado.

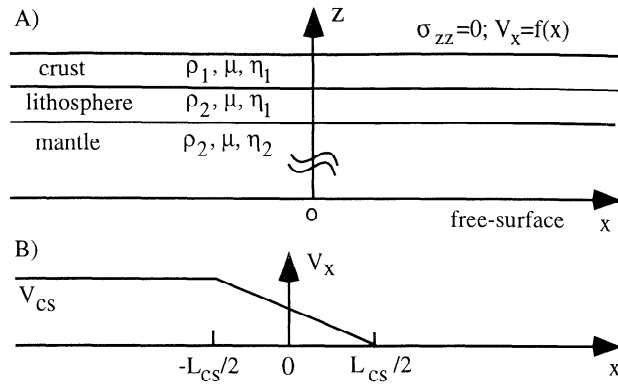


Figure 1. (A) Schematics of crustal compensation models. The depths of the Moho and the base of the lithosphere are 35 km and 100 km, respectively. The densities of crust and mantle are 2800 kg m^{-3} and 3300 kg m^{-3} . The models assume for the crust and mantle a shear modulus of $1.5 \times 10^{11} \text{ Pa}$ and Poisson's ratio of 0.5. (B) The distribution of surface velocity $V_x(x)$. Parameters V_{cs} and L_{cs} are 3 cm yr^{-1} and 1000 km.

This study extends our past analysis [Zhong, 1997] in that we consider the effect on the evolution of isostasy of active crustal convergence. Crustal shortening is applied through a horizontal velocity boundary condition on the surface (Figure 1). The vertical stresses on the surface set to zero so that surface topography can be tracked. The surface, Moho, and lower boundary of the model are assumed to be initially flat.

Our model assumptions warrant discussion. In practice, crustal deformation is accommodated mainly through brittle deformation above seismogenic zones. However, in contrast to deformation of oceanic plates which is concentrated along plate margins, continental deformation over active orogenic belts tends to be distributed over areas as wide as 1000 km [England and Molnar, 1997]. Therefore, if temporal and spatial scales are sufficiently large in comparison to the corresponding scales for brittle deformation (i.e., averaged period of earthquake cycles and separation between faults) on continents, the brittle deformation to the first order may be approximated as deformation within a simple viscous medium. With such an approximation, the viscosity can only be interpreted as the effective viscosity averaged over the temporal and spatial scales of brittle deformation [England and Molnar, 1997]. In our models, the driving force for mountain-building is the horizontal boundary velocity (Figure 1), and the velocity boundary condition is assumed not to vary with time. This assumption should be valid when the external force leading to crustal convergence dominates over the gravitational body force associated with the mountain belts during active orogeny. The gravitational force may become important enough to cause the spreading and collapse of mountain belts subsequent to mountain building [Bird, 1989].

Results

We have explored illustrative models relevant to areas of large-scale crustal shortening. Case 1 consists of a 100-km thick lithospheric layer with viscosity of 10^{22} Pa s that overlies a weaker mantle layer with a viscosity of 10^{21} Pa s . The mantle viscosity of 10^{21} Pa s is consistent with the average mantle viscosity deduced from glacial rebound studies [e.g., Cathles, 1975]. Figure 2A shows profiles of surface and

Moho topography after 3, 11, and 20 million year (Ma) crustal convergence. The surface elevates to form a plateau in regions where the crust converges, while the Moho boundary depresses to form a mountain root (Figure 2A). To examine the compensation process, we decompose these surface and Moho topographic profiles in a spectral domain and compute degree of compensation D_c for each wavelength. The value of D_c for each wavelength is

$$D_c = -\frac{H_{moho}\Delta\rho_{moho}}{H_{surf}\Delta\rho_{surf}}, \quad (5)$$

where H_{surf} and H_{moho} are the surface and Moho topography at the given wavelength, and $\Delta\rho_{surf}$ and $\Delta\rho_{moho}$ are the density differences at the surface and Moho boundaries. $D_c=1$ for the Airy isostasy. For $D_c<0$ and $D_c>0$, the surface and Moho boundaries display characteristics of folds and boudinage structure, respectively. At 3 Ma, D_c significantly exceeds unity for wavelengths shorter than 1000 km (Figure 2B; because the convergence is symmetric at $x=0$, the amplitude of spectra for topography is zero at even wave-numbers), indicating that the crust greatly deviates from the Airy isostasy. Figure 2B shows that as time increases, D_c approaches unity for all the wavelengths greater than 200 km. The value does not change much from 11 to 20 Ma, which indicates that significant compensation occurs in the relatively early stage of crustal shortening. Since the power in the surface and Moho topography at 20 Ma is distributed primarily at wavelengths longer than 500 km, D_c indicates that the crust is nearly compensated (Figure 2B).

It is important to realize that while the amplitude and shape of the topography depend on the boundary velocity (i.e., V_{cs} and L_{cs} in Figure 1), the dependence of D_c on wavelength at a given time only depends on the viscoelastic property of our models (i.e., the relative viscosity contrast between lithosphere and mantle) [Zhong, 1997]. At a given time, the amplitude of topography is influenced by V_{cs} and L_{cs} ; the larger V_{cs} is or the smaller L_{cs} , the larger the amplitude of topography. For a given material property, the power spectra of the surface and Moho topography at a given time are determined by L_{cs} and can be linearly scaled with V_{cs} . For example, with the same mechanical property model as in Case 1, if a small L_{cs} is chosen such that the power of the topography is concentrated near 200 km wavelength, the crust will be largely over-compensated (i.e., $D_c>1$) 20 Ma after the crustal shortening (Figure 2B).

We now investigate the effects of a high lithospheric viscosity. Case 2 differs from Case 1 in only having a higher viscosity (10^{23} Pa s) for the lithosphere including the crust. Figure 2C shows that in the early stage (e.g., 3 Ma), the surface and Moho topography grow to form folds with elevated topography outside of the regions where crustal shortening occurs, and subsequently, the folding structure decays and turns into boudinage structure. At 20 Ma, the surface and Moho topographic profiles are similar to those in Case 1, although the surface topography in Case 1 shows more plateau-like features (Figures 2A and 2C). Figure 2D shows that D_c at 3 Ma is negative for wavelengths smaller than 2000 km, indicative of folding at these wavelengths and significant departure from the isostasy. As time increases, the range of wavelengths over which D_c is negative decreases, and the wavelength at which Airy isostasy (i.e., $D_c=1$) is achieved decreases. At 20 Ma, D_c becomes positive for all wavelengths, and D_c is close to

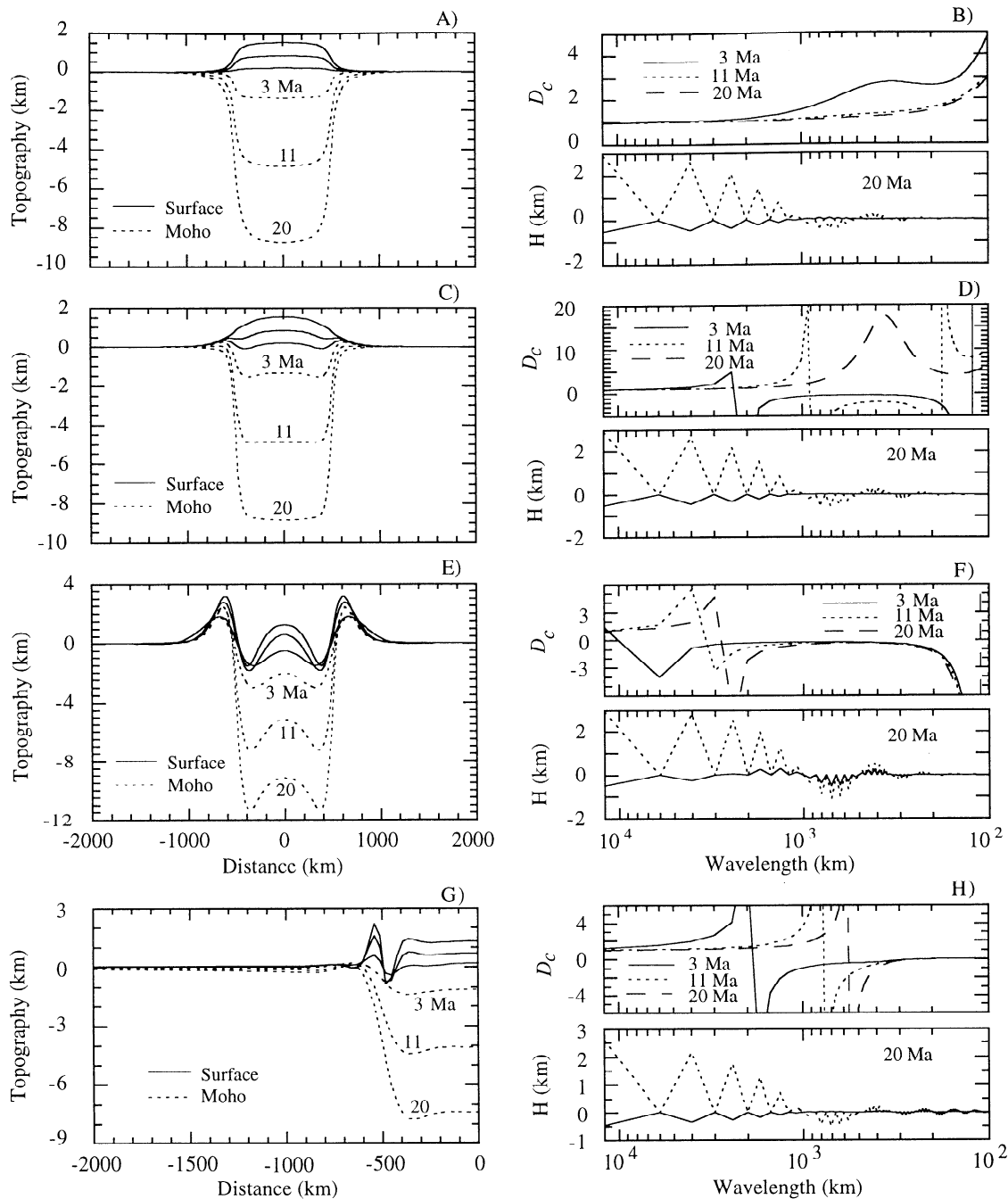


Figure 2. Profiles of surface and Moho topography (A), wavelength-dependence of D_c (the top panel of B) at different times, and the topography spectra H at 20 Ma (bottom panel of B; solid and dashed lines are for surface and Moho topography, respectively) for Case 1, and the corresponding results for Cases 2 (C and D), 3 (E and F), and 4 with different viscosity for continental lithosphere. In (G), only half of the profiles is shown. The ratios of lithospheric to mantle viscosities are 10, 10^2 , and 10^3 for cases 1, 2, and 3, respectively. Case 4 includes a weak lower crust.

1 for all the wavelengths over which the surface and Moho topography have a significant power.

As for the degree of compensation, the timings of growth and decay of folds primarily depend on the viscosity contrast between lithosphere and mantle. In Case 3, continental lithospheric viscosity is further increased to 10^{24} Pa.s. Figure 2E illustrates that the surface at the early stage (3 Ma) subsides in the central region of crustal shortening, and the crust develops more prominent folds. Subsequently, the surface

slowly rebounds, while the Moho continues to subside. As a result, D_c at 20 Ma remains negative for wavelengths shorter than 2500 km, which corresponds to the folding mode of deformation (Figure 2F). At 20 Ma, there is significant power of the surface and Moho topography over these wavelengths (i.e., <2500 km) (Figure 2F), indicating that the crust deviates significantly from the Airy isostatic state.

It has been suggested that the lower crust may be weaker than lithospheric mantle and the upper crust [Brace and

Kohlstedt, 1980]. Effects of a weak lower crust on some aspects of crustal deformation are examined in [Kusznir and Matthews, 1988; Bird, 1989; Royden, 1996]. In Case 4, the lower crust (from 20 km to 35 km in depth) is assumed to have a viscosity of 10^{21} Pa·s, and Case 4 is otherwise identical to Case 3. Figure 2G shows that for this case with a weak lower crust, the Moho is depressed over a larger distance with smaller amplitude, compared with previous cases. The surface topography in Case 4 shows a plateau at the center of crustal convergence (i.e., at $x=0$) but modulates at the edge of the plateau at a wavelength of about 200 km. This 200 km wavelength is much smaller than that from Case 3 (Figure 2E), reflecting the reduced thickness of the strong top layer. This dependence of folding wavelengths on layer thickness is similar to that found in previous studies [e.g., Zuber and Parmentier, 1996].

Degree of compensation (Figure 2H) shows that the crust at 3 Ma is over-compensated (i.e., too large Moho depression) from 2000 km to 10^4 km wavelengths. As time increases to 20 Ma, the crust reaches approximately isostasy for wavelengths larger than 1000 km (Figure 2H). However, for wavelengths less than 1000 km, D_c significantly deviates from unity with zero for wavelengths less than 300 km (Figure 2H). The weak lower crust makes it difficult for the Moho to support short wavelength (<300 km) topography, while with the strong upper crust, the surface develops significant topography at these wavelengths (Figure 2H), resulting in D_c which is near zero at small wavelengths in Figure 2H.

Discussion and Conclusions

Our models (Cases 1, 2, and 3) show that if continental lithosphere is approximated as a homogeneous layer and if the effective viscosity of lithosphere is no more than 100 times of that of the underlying mantle, crustal shortening would produce approximately isostatic orogenic belts within twenty million years of convergence (Figures 2A and 2C). Continental lithosphere that is too strong results in crust-scale folds under the influence of crustal convergence. Models with a relatively weak lower crust bounded by strong upper crust and lithospheric mantle (Case 4) indicate that the crust may still significantly deviate from the isostatic state for wavelengths as large as 1000 km, although over a broader range of wavelengths the crust reaches the isostasy (Figure 2H).

It should be pointed out that our analytic models ignore faulting, nonlinear rheology, and heterogeneity in lithospheric strength, and this could have some effects on the folding in Cases 3 and 4 (Figures 2E and 2G). Faulting and nonlinear rheology tend to introduce lateral variations in lithospheric viscosity by weakening lithosphere where the stress is high. Therefore, in actuality, the folds in Cases 3 and 4 may turn into thrust fault belts or zones of weakness, and they may not fully develop. However, we believe that this will not significantly change our main conclusion.

Despite of the simplifications invoked in our models, the implications of our results are obvious. For active and young orogenic belts with characteristic widths greater than 200 km (or wavelengths greater than 400 km) that are approximately isostatically compensated, the effective viscosity for continental lithosphere in average can be no more than 100 times of the viscosity of the underlying mantle viscosity. The effective viscosity of continental lithosphere inferred from

measured strain rates in Tibetan plateau and Tian Shan regions is only 10 to 100 times larger than the underlying convective mantle viscosity [England and Molnar, 1997]. Because both Tibetan plateau and Tian Shan are approximately isostatically compensated, as suggested by regional gravity studies [Jin et al., 1996; Burov et al., 1990], the relatively small continental viscosity inferred for these regions is consistent with our model predictions.

Acknowledgements: This work was supported by the NASA Planetary Geology and Geophysics Program. We thank A. Lenardic for reviewing the paper.

References

- Abdrakhmatov, K. Ye, S. A. Aldazhanov, B. H. Hager, M. W. Hamburger, T. A. Herring, K. B. Kalabaev, V. I. Makzrov, P. Molnar, S. V. Panasyuk, M. T. Prilepin, R. E. Reilinger, I. S. Sadybakasov, B. J. Souter, Yu. A. Trapeznikov, V. Ye. Tsurkov, and A. V. Zubovich, Relatively recent construction of the Tien-shan inferred from gps measurements of present-day crustal deformation rates, *Nature*, 384, 450-453, 1996.
- Bird, P., Lateral extrusion of lower crust from under high topography in the isostatic limit, *J. Geophys. Res.*, 96, 10275-10286, 1991.
- Brace, W. F., and D. L. Kohlstedt, Limits on lithospheric stress imposed by laboratory experiments, *J. Geophys. Res.*, 85, 6248-6252, 1980.
- Burov, E. V., M. G. Kogan, H. Lyon-Caen and P. Molnar, Gravity anomalies, the deep structure, and dynamic processes beneath the Tien Shan, *Earth Planet. Sci. Lett.*, 96, 367-383, 1990.
- Cathles, L. M., *The viscosity of the Earth's mantle*, 386, Princeton Univ. Press, Princeton, N. J., 1975.
- Daly, R. A., *Strength and structure of the Earth*, 434, Prentice-Hall, Englewood Cliffs, 1940.
- Dewey, J. F. and K. C. A. Burke, Tibetan, Variscan, and Precambrian basement reactivation: Products of continental collision, *J. Geol.*, 81, 683-692, 1973.
- England, P., and P. Molnar, Active deformation of Asia - from kinematics to dynamics, *Science*, 278, 647-650, 1997.
- England, P., and D. McKenzie, A thin viscous sheet model for continental deformation, *Geophys. J. R. Astro. Soc.*, 70, 295-321, 1982.
- Fleitout, L. and C. Froidevaux, Tectonics and topography for a lithosphere containing density heterogeneities, *Tectonics*, 1, 21-56, 1982.
- Houseman, G., D. P. McKenzie, and P. Molnar, Convective instability of a thickened boundary layer and its relevance for the thermal evolution of continental convergent belts, *J. Geophys. Res.*, 86, 6115-6132, 1981.
- Jin, Y., M. McNutt, and Y. S. Zhu, Mapping the descent of Indian and Eurasian plates beneath the Tibetan plateau from gravity anomalies, *J. Geophys. Res.*, 101, 11275-11290, 1996.
- Kusznir, N. J. and D. H. Matthews, Deep seismic reflections and the deformational mechanics of the continental lithosphere, *J. Petrol.*, Special Issue, 64-87, 1988.
- McNutt, M., Implications of regional gravity for state of stress in the Earth's crust and upper mantle, *J. Geophys. Res.*, 85, 6377-6396, 1980.
- Molnar, P. and P. Tapponnier, Cenozoic tectonics of Asia: Effects of a continental collision, *Science*, 189, 419-426, 1975.
- Royden, L., Coupling and decoupling of crust and mantle in convergent orogens: Implications for strain partitioning in the crust, *J. Geophys. Res.*, 101, 17,679-17,705, 1996.
- Zhong, S., Dynamics of crustal compensation and its influences on crustal isostasy, *J. Geophys. Res.*, 103, 6377-6396, 1997.
- Zuber, M. T., and E. M. Parmentier, Finite amplitude folding of a continuously viscosity stratified lithosphere, *J. Geophys. Res.*, 101, 5489-5498, 1996.